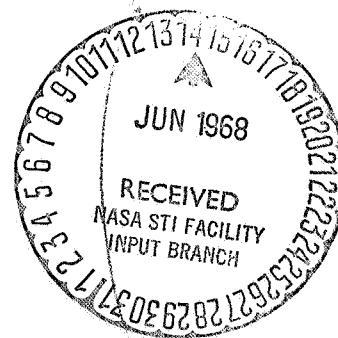


## FM/AM TELEMETRY TO MEASURE IMPACT ACCELERATIONS

Dean R. Harrison  
Research Scientist  
Ames Research Center, NASA  
Moffett Field, Calif. 94035



### ABSTRACT

An FM/AM telemetry system has been designed which provides three-axis acceleration measurements during impact tests of models of soft-landing structures. The system was designed to employ a three-axis piezoelectric accelerometer working into three separate FM/AM telemeter circuits. Each carrier was received and detected by a separate receiver at the ground station. The subcarrier output of the receiver was recorded directly on magnetic tape. The frequency of the subcarrier was preset to the center frequency of the tape recorder FM-reproduce electronics to facilitate demodulation of the recorded subcarrier during playback of the tape. During calibration drop tests acceleration wave forms were recorded by both telemetry and direct wire techniques. Wave-form comparisons showed close correlation for each axis tested.

### INTRODUCTION

Many useful techniques for obtaining free-flight aerodynamic characteristics in gun ranges and wind tunnels have been developed in recent years. The requirements of test conditions, miniaturization, multichannel capability and high "g" reliability have necessitated the development of special telemetry circuits, transducers and techniques for telemetering various parameters on free-flight models.

Most of the previous problems related to aerodynamic measurements on models pertain to the behavior of the model in free flight. The present problem is that of obtaining an accurate three-axis measurement of the impact accelerations of the model at the end of the flight.

Telemetry for free-flight gun ranges and wind-tunnel tests has been developed and reported in the literature. Piezoelectric,<sup>1,2</sup> piezoresistive,<sup>3</sup> and capacitive type<sup>4,5</sup> accelerometers have been employed for aerodynamic measurements. The gun-range work reported by CARDE suggested an FM/FM frequency multiplexing telemetry system for multichannel force measurements by piezoelectric accelerometers, but to date a fully developed system has not been reported in the literature.

Telemetry was used so that the model would be free of any constraint during impact. The system is designed to withstand high g impact and to provide (a) a continuous record during the event to determine the envelope of the acceleration-time

Superior numbers refer to similarly-numbered references at the end of this paper.

curve; (b) resolution of the x, y, and z axis components, (c) good time correlation between axes, and (d) a data format suitable for use with automatic processing systems.

The system employs a three-axis piezoelectric accelerometer working into three separate FM/AM telemeter circuits (Fig. 1). Each carrier is received and detected by a separate broad-band telemetry receiver at the ground station. The subcarrier output from the receiver is recorded directly on magnetic tape. The frequency of the subcarrier is preset to the center frequency of the tape-recorder FM-reproduce electronics to facilitate demodulation of the recorded subcarrier while the tape is played back.

The system performance is evaluated by calibration drop tests in which data are collected by both telemetry and direct wire. Wave forms from both systems are presented for visual comparison.

### TELEMETRY SYSTEM

#### Three-Axis Accelerometer

A commercially available accelerometer provided a nominal sensitivity of 5 mV/g for each of three orthogonal axes and a range of 0 to 1000 g.

#### Telemeter Circuit

During an initial attempt to design an FM/FM telemetry system, it was found that because the proximity of the three telemeter circuits, they were susceptible to carrier-frequency pulling, which caused excessive channel cross talk. By comparison, the FM/AM system, described below, showed none of the undesirable cross-talk effects.

A sketch of the FM/AM telemetry circuit finally used is shown in Fig. 2. The circuit consists of a voltage follower ( $Q_1$ ), ( $Q_2$ ) which uses a boot-strap circuit to provide an input impedance greater than 300 M $\Omega$ . The output of the voltage follower is coupled through a 68 k $\Omega$  resistor and a PNP emitter follower,  $Q_3$ , to the input of the subcarrier oscillator. The 68 k $\Omega$  resistor sets the voltage sensitivity of the subcarrier voltage controlled oscillator (VCO). The PNP follower improves the frequency stability of the VCO. Deviation is provided by the incoming signal applied to the base of  $Q_5$  and  $Q_7$ . A frequency deviation of  $\pm 40\%$  produces full-scale output from the recorder during playback. The inherent linearity of multivibrator VCO circuit during wide deviations in frequency is further improved by the addition of transistors  $Q_4$  and  $Q_6$ , which also improves the turn-on reliability of the

N68-34442  
(ACCESSION NUMBER)

(THRU)

11  
(PAGES)

1  
(CODE)

TMX 61204  
(NASA CR OR TMX OR AD NUMBER)

14  
(CATEGORY)

circuit. However, the main purpose of these transistors is to reduce the rise time of the multi-vibrator. The square wave output is coupled from the collector of  $Q_7$  to a buffer transistor  $Q_8$  which is normally biased below cutoff. This buffer isolates the subcarrier oscillator from the load of the transmitter stage. The final stage  $Q_9$  is normally biased below cutoff and is switched on and off by the incoming square wave. This type of amplitude modulation, sometimes referred to as carrier keying, assures 100% modulation of the carrier at all times. Shown in figure 3 are the wave forms at (a) the collector of  $Q_7$  in the subcarrier oscillator, (b) the output of the receiver I.F. amplifier, and (c) the receiver video output which is normally recorded on the tape recorder.

The inductance of the RF stage functions as a tuning element and the radiating antenna. RF carrier shift was not a problem during these tests because of the method of carrier modulation and the bandwidth of the receiver. In applications where loss of the carrier may occur as a result of proximity detuning, the carrier can be crystal stabilized with high-g RF crystals.<sup>6</sup> Crystal stabilization of an FM/AM system has been used successfully in biomedical telemetry implants.<sup>7,8</sup>

To summarize, the completed telemetry circuit provided a 300 M $\Omega$  input impedance for the piezoelectric transducer. Input signals of the order of  $\pm 1$  V provided a linear deviation in the 54 kHz subcarrier oscillator of  $\pm 40\%$ . The carrier frequency was adjustable from 90 to 147 MHz, and was 100% amplitude modulated.

#### Fabrication

The three-channel telemetry package, including the three-axis telemetry, is shown in Fig. 4. Also shown are the mercury battery pack and a telemetry circuit prior to potting. The main body of the package is a 2-in.-diameter cylinder of polycarbonate plastic, 1-1/2 in. long. The body is machined to accommodate a battery pack in the center. Four recesses equally spaced around the battery accommodate the telemetry circuits which are held in place by nonconducting screws. After the final frequency adjustments are made, on all three telemetry circuits, potting compound, Solithane 113 formulation 15, is injected into the recess containing the telemetry to firmly support the components. The tensile strength of the potting formulation is 3200 psi. Significant electrical properties of the potting formulation are: a dielectric constant of 2.8, a dissipation factor of 0.004, a volume resistivity of  $3.6 \times 10^{14}$   $\Omega$ -cm, and a surface resistivity of  $1.5 \times 10^{15}$   $\Omega$ . The potted unit was hard but not brittle. In some cases it was possible to cut through the potting with a knife to repair damaged units.

After the potting, a printed circuit board containing battery connections for each telemetry circuit was screwed to the top of the package. The accelerometer was then mounted on the top of the printed circuit and firmly screwed to the polycarbonate body. The accelerometer and each circuit were connected by shielded coaxial cable. The input impedance of 300 M $\Omega$  and the subcarrier frequency were

unaffected by the potting compound, but the carrier frequencies dropped (by 6 to 10 MHz) as expected. The effect on the radiated power was negligible. The total weight of the completed package is 168 grams.

#### Electrical Characteristics

(a) Voltage sensitivity. Each channel provided a sensitivity of approximately  $\pm 1$  V output at the recorder for a  $\pm 1$  V input at the telemetry input (Fig. 5). The sensitivity of any particular channel to acceleration input was controlled by the shunt capacitance across the input and could be adjusted according to the test requirements. A drop tester was normally used for acceleration sensitivity calibrations.

(b) Linearity. System linearity was obtainable by either a voltage calibration or by the acceleration drop test. In Fig. 6 is shown a pair of oscillograph traces for a qualitative comparison of the linearity obtained by a voltage source. The signal input was a triangular wave of 1 kHz. The output is rounded, and shifted in phase, but otherwise appears linear. Nonlinearity was determined to be in the order  $\pm 10$  mV for a  $\pm 1$  V output, or of the order of 1%.

(c) Stability of the SCO. Temperature stability tests of the subcarrier oscillator from 0°C to 65°C indicated a typical drift of the order of 0.15% of full-scale deviation per °C. In each case the observed drift was in the same direction, indicating that further compensation could improve the stability. No further effort was made in this regard since variations in test temperatures were never more than  $\pm 10^\circ\text{C}$  and this produced a negligible change in subcarrier frequency. The subcarrier voltage stability was found to be typically 1% of full scale deviation per volt drop in battery voltage. To date, no instability in the subcarrier has been observed as a result of g loading up to 3000 g.

(d) Cross-talk. Cross talk between channels, exclusive of the three-axis accelerometer, is below the output noise level.

(e) Signal-to-noise levels. Fig. 7 is a plot of the signal-to-noise ratio in dB (referenced to full-scale output of the system) measured with a true RMS voltmeter as a function of receiver signal strength.

(f) Phase response. A linear phase response for each channel and a minimum phase shift between channels is necessary to provide an undistorted output and good time correlation between channels. Fig. 8 is a phase response curve plotted on a linear scale. The linear variation is typical of all channels measured and can be attributed to the characteristic of the filter on the tape recorder FM discriminator output. In other words, the telemetry circuit produces no phase shift of its own over the range of frequencies tested. Phase differences of several degrees for the equipment used were observed when the subcarrier frequency of the telemetry was not identical to the center frequency of the tape recorder FM discriminator, and when the FM

discriminator output was unsymmetrical or nonlinear. When frequencies of the subcarrier and discriminator were properly aligned and the discrimination was properly adjusted, the difference in phase response between channels was of the order of a half degree.

(g) Frequency response. The low frequency cutoff (-3 dB) of the accelerometer is limited by the input impedance of the amplifier and is computed from  $fR_{in}C_{total} = 0.16$ . The peak input voltage to the amplifier must be limited to  $\pm 1$  V. Thus, the shunt capacitance necessary to develop this voltage can be determined at a specific "g" level and accelerometer sensitivity. A value of 5000 pF was frequently required. Since the input impedance was 300 M $\Omega$ , a low frequency cutoff of 0.1 Hz was expected. However, the actual 3 dB point was 0.5 Hz due to the additional effect of the output coupling capacitor of the voltage follower circuit. The upper frequency cutoff of 8.8 kHz is the upper limit of the tape recorder electronics. Playing back the tape into a high performance discriminator could substantially improve the upper frequency cutoff and linearity if needed.

(h) Power requirements. A 6.7 V mercury battery pack with a 250 mA-hr capacity supplied power for all three telemetry circuits. Under normal conditions, the total circuit drain was approximately 5 mA, providing a 40 to 50 hour life.

#### Receiving Station

Three  $3\lambda$  vertical dipole antennas were spaced around the test site within 10 feet of the impact point, with one end near a conducting ground plane. This arrangement gave a signal strength of approximately 100  $\mu$ V at each of the three receivers.

The telemetry receivers provided a  $\pm 750$  kHz video bandwidth which was adequate for the undistorted processing of the 54 kHz subcarrier square wave. Sufficient bandwidth to allow faithful reproduction of the leading and trailing edges of the square wave contributed significantly to the high signal-to-noise ratio of the system. The tape recorder allowed simultaneous recording and playback of the telemetry data, a timing signal and other test parameters of interest. The square wave output of the receiver was recorded in the direct-record mode and played back in the FM reproduce mode. In this manner the tape recorder discriminator was used to demodulate the frequency-modulated subcarrier. The speed of the recorder playback could be adjusted to be compatible with an analog-to-digital recording system to facilitate the data reduction process. Also the analog output of the tape recorder discriminator could be recorded on an oscillograph or displayed on an oscilloscope for quick-look evaluation.

#### Calibrations

Figure 9 is a photograph of the drop-test calibration apparatus. A laminated balsa-wood block was bored out to hold the telemetry package. The block was oriented according to the axis to be tested and mounted on the metal test table.

The test procedure involved at least two drops from each height. In the first drop, the three-axis accelerometer output was disconnected from the telemetry circuit and directly wired to a readout system normally used with a reference accelerometer mounted on the test table. This drop provided a measurement of the accelerations undergone by the accelerometer mounted directly on the telemeter package. The second drop was performed with the telemeter circuit connected to the accelerometer. Assuming that the apparatus provides repeatable accelerations, then relating the telemetered data to the data from the direct-wired calibrated accelerometers provides a system calibration. Typical data obtained in this manner are shown in Fig. 10. The repeatability of acceleration levels in succeeding drops was approximately  $\pm 3\%$ . A sample of waveforms obtained for the calibrations described is shown in Fig. 11. The envelopes of corresponding waveforms correlate reasonably well. The damped oscillations observed on the x and y axes result for the resonance of a cantilever support used in attaching the telemeter to the drop-test equipment.

#### Test Facility.

Figure 12 is a simplified diagram of the test apparatus which is located in a vacuum tower 100 feet tall and 26 feet wide. The pneumatic launcher directs a mass downward, providing impact against the model which is suspended near floor level. Velocity timing stations, motion picture cameras, and other instrumentation are not shown. The test section pressure and temperature for the test described below are 5 mm Hg and room temperature, respectively.

#### Impact Tests

Initial impact tests were made so that the telemetry output could be compared with direct wire output of a second accelerometer mounted in the model. That is, the model containing the telemetry and direct wire accelerometer was located in front of the launcher. A mass was then fired from the launcher into the model thus providing rapid acceleration. The test provided data which allowed direct comparisons of waveforms and magnitudes of telemetered and direct-wired data. The waveforms of the Z-axis acceleration measured by the two systems, as shown in Fig. 13, correlate in time and magnitude. The noise spikes that occurred prior to impact could have resulted from either an inadequately shielded input lead to the source follower or insufficient video amplitude from the receiver to drive the tape recorder limiter into saturation. Both problems have been corrected in the most recent package, as shown in Fig. 11, by the clean traces obtained during the calibration drop tests. The x- and y-axis data did not show the quality of correlation obtained in the Z axis. The reason is believed to be a result of inadequate alignment of the corresponding axis on the accelerometers, difference in the position of the accelerometers within the model, and differences in mounting structures.

## SUMMARY

A three-axis accelerometer with separate, noninterfering telemetry has been used to measure acceleration during impact. The performance requirements of time correlation between axes, linearity, sensitivity and signal-to-noise ratio are met by use of an FM/AM telemetry system, and piezoelectric accelerometers. The calibration accuracy is estimated at  $\pm 5\%$  and believed to be limited by the calibration technique and not the system.

## ACKNOWLEDGEMENTS

The author would like to express a sincere thanks to Messrs. G. J. Deboo and T. B. Fryer of Electronics Research Branch and to L. R. Guist of the Structural Dynamics Branch for their many helpful suggestions.

## REFERENCES

1. Letarte, M. and Moir, L. E., "A High g Telemetry System for Gun and Rocket Firing." Canadian Armament Research and Development Establishment. Valcartier, Quebec, Report No. TM 351/60, August 1960.
2. Mermagen, W. H., "High g Telemetry for Ballistic Range Instrumentation." Ballistic Research Laboratories, Memorandum Report No. 1566, April 1964.
3. Trapp, D. L., "A Miniaturized RF Acceleration Measuring System." Proc. International Telemetering Conference, Los Angeles, Calif., Vol. 2, Oct. 1966.
4. Harrison, D. R., Coon, G. W., Mateer, G. G., and Peterson, V. L., "FM Telemetry For Multiple Force Measurements on Free-Flying Models in Wind Tunnels." Proc. of the 2nd International Congress on Instrumentation in Aerospace Simulation Facilities, Aug. 1966, Stanford Univ., Republished in IEEE Trans. AES, Vol. AES-4, No. 2, March 1968.
5. Holley, J. A., and Hayes, D., "Hardened Technology Study Ballistic Range Instrumentation Report." Lockheed Report No. Y-75-65-L, Contract A.F. No. 04(695)-655, June 1965.
6. Liss, F. T. and Richardson, J. F., "Ruggedized Quartz Oscillator Crystals for Gun-Launched Vehicles." Proc. International Telemetering Conference, Washington, D. C., Vol. 3, Oct. 1967.
7. Kurtenback, A. J. and Dracy, A. E., "The Design and Application of an FM/AM Temperature Telemetering System for Intact, Unrestrained Ruminants." IEEE Trans. Bio-Medical Engineering, Vol. BME-12, Nos. 3 and 4, July/Oct. 1965.
8. Zweizig, J. R., Kado, R. T., Hanley, J., and Adey, W. R., "The Design and Use of an FM/AM Radio Telemetry System for Multichannel Recording of Biological Data." IEEE Trans. Bio-Medical Engineering, Vol. BME-14, No. 4, Oct. 1967.

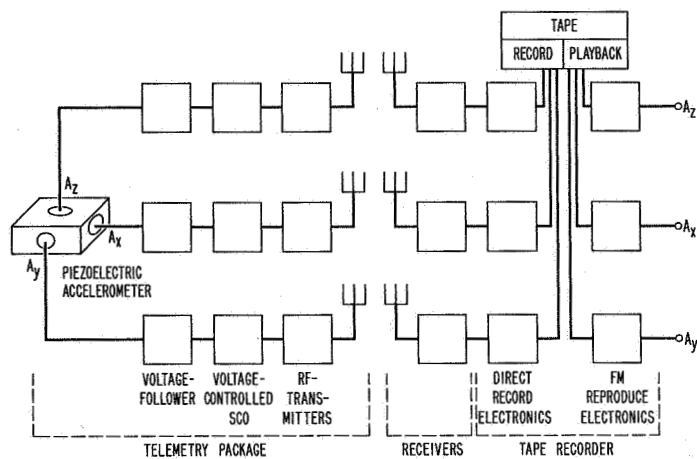


Fig. 1 Sketch of FM/AM impact telemetry system.

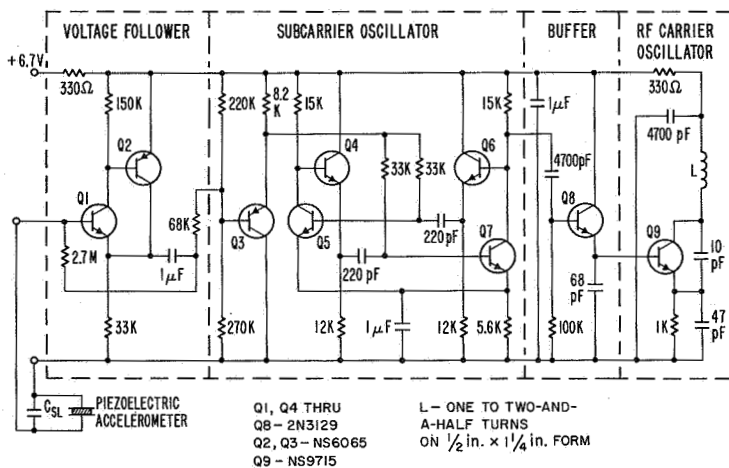


Fig. 2 Circuit diagram of FM/AM transmitting electronics.

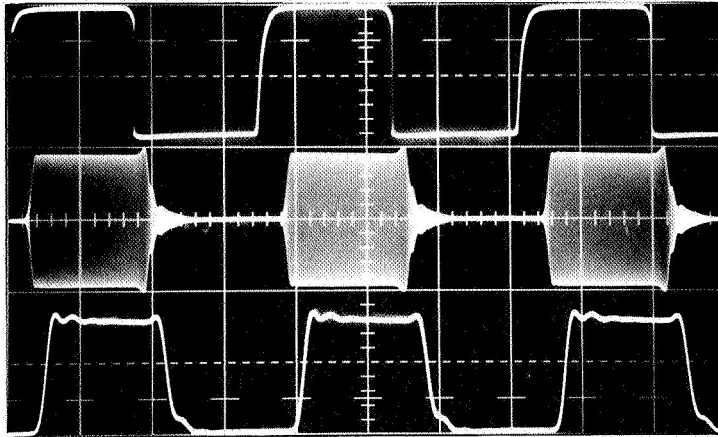


Fig. 3 An oscillograph of the VCO output (top trace), the modulated carrier (middle trace), and the detected video output (bottom trace). Sweep speed:  $5 \mu\text{s}/\text{cm}$ .

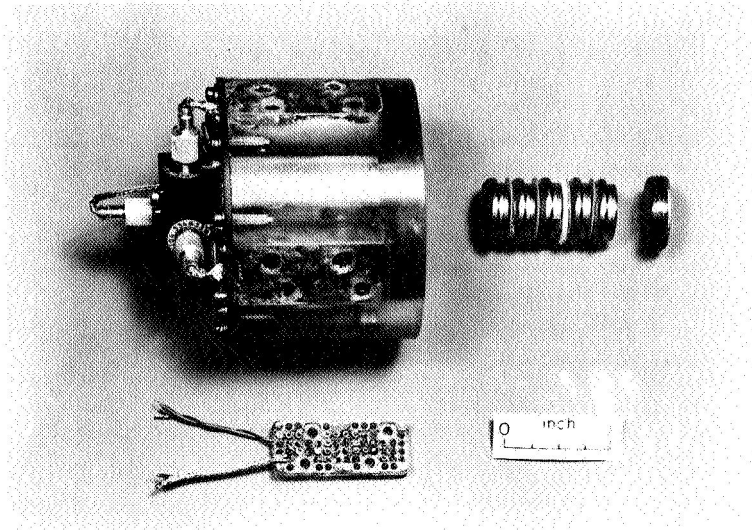


Fig. 4 The FM/AM telemetry package, battery pack, and an unpotted telemetry circuit.

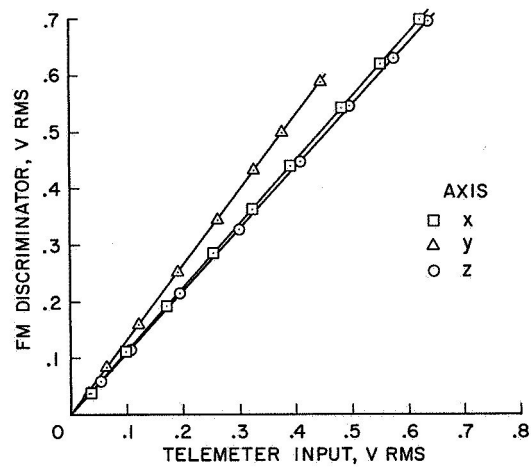


Fig. 5 Voltage calibration of telemetry system for three channels.

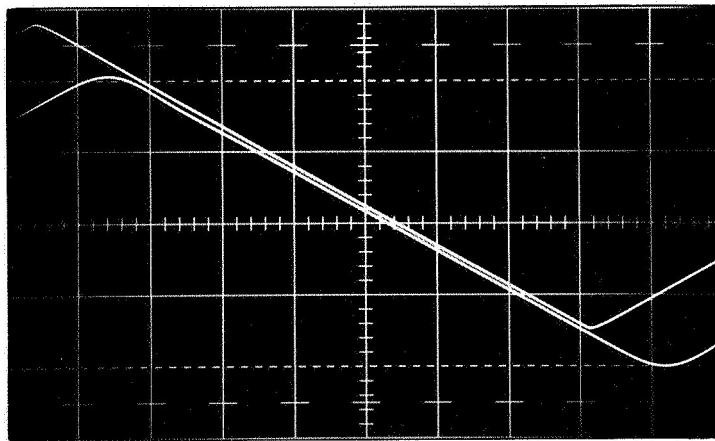


Fig. 6 Oscilloscope traces demonstrating system linearity. Top trace: Input voltage, vertical scale: 0.53 V/cm. Bottom trace: System output voltage, vertical scale: 0.5 V/cm. Sweep speed: 50  $\mu$ s/cm.

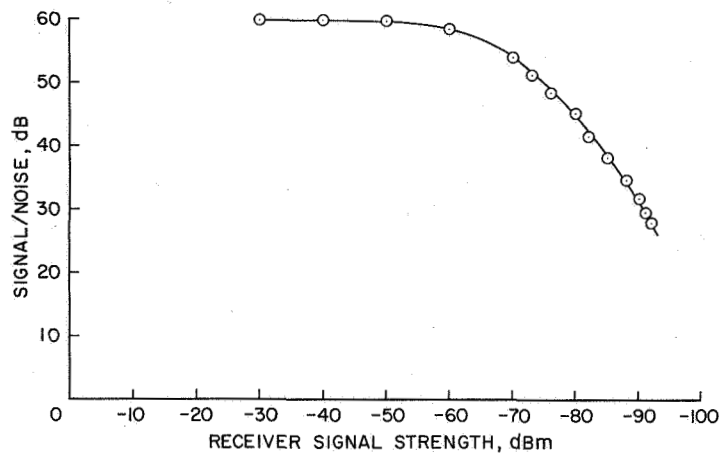


Fig. 7 Signal-to-noise ratio of the FM/AM system as a function of receiver signal strength. Filtering: receiver IF, 3 MHz; receiver video, 750 kHz; tape recorder FM disk, 10 kHz.

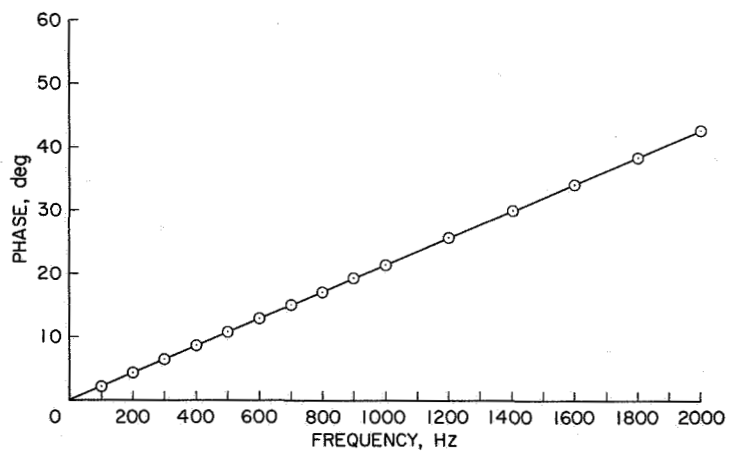


Fig. 8 System phase response.



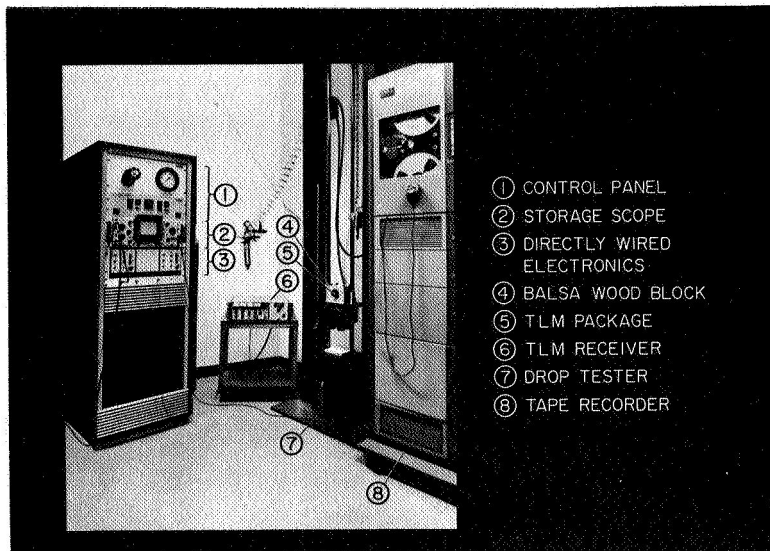


Fig. 9 Drop-test calibration apparatus and instrumentation.

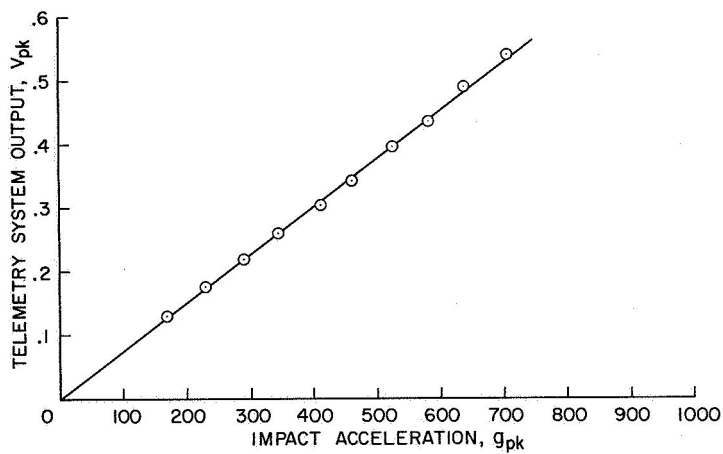


Fig. 10 Acceleration calibration of the telemeter system for one axis.

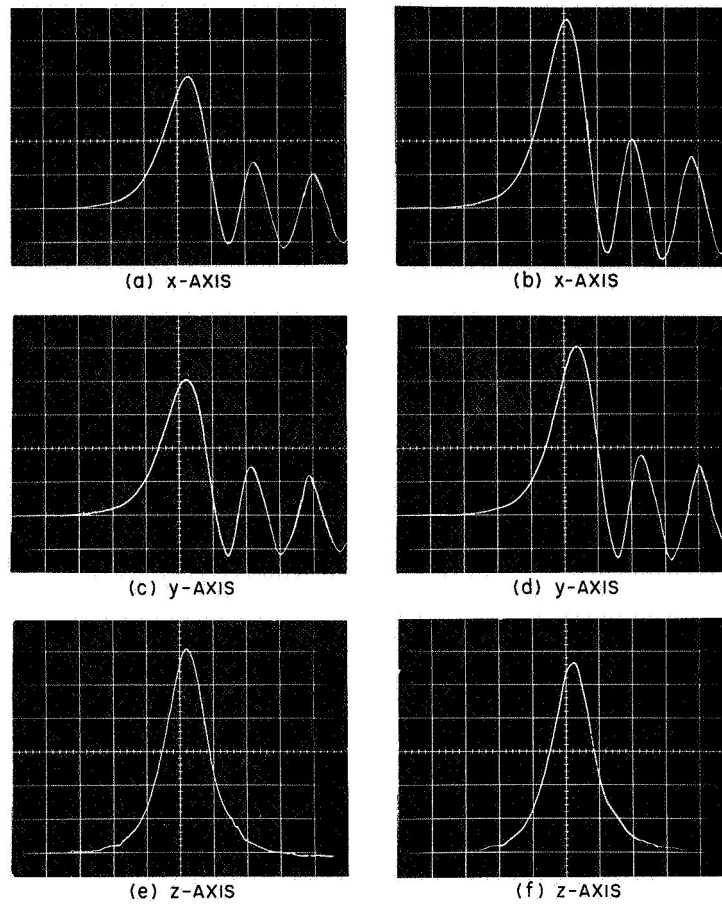


Fig. 11 Telemetered (a, c, and e) and direct wire (b, d, and f) acceleration traces. Sweep speed: 0.5 msec/cm, vertical (a, c) 0.2 V/cm (e) 0.0685 V/cm; (b, d, and f) 100 g/cm.

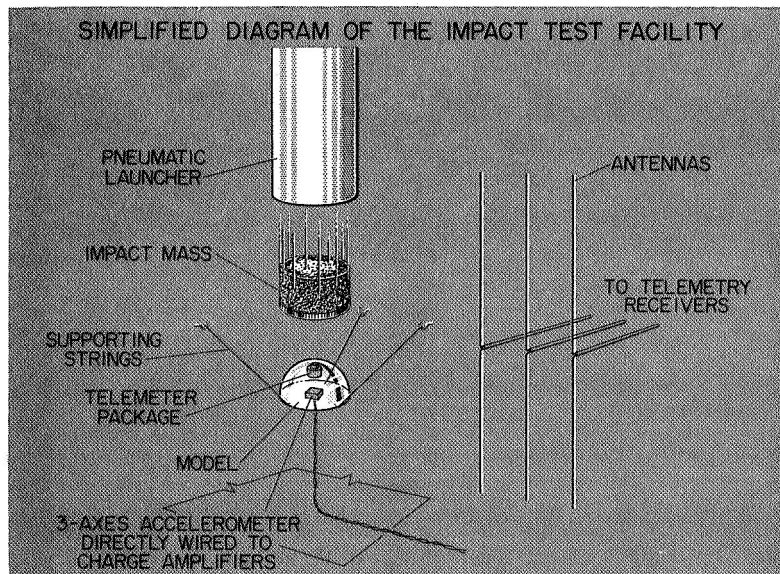


Fig. 12 Simplified diagram of the impact test facility.

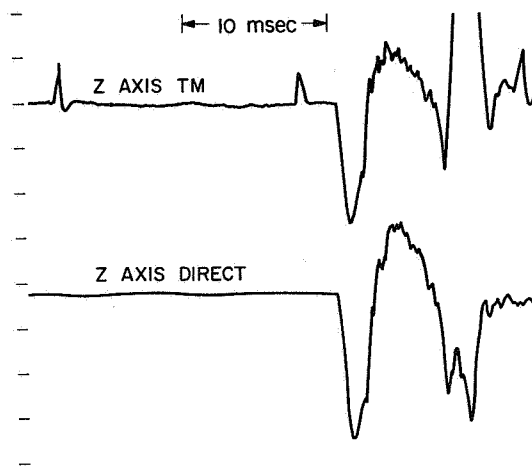


Fig. 13 Telemetered and direct wire acceleration measurements.